# Evaluation of Head and Cervical Spine Kinematics of GHBMC M50-O and THUMS AM50 Occupants in Moderate-Speed Rear Impact

Timothy DeWitt, Vikram Pradhan, Yun-Seok Kang

***Abstract*** The current study evaluates the Total Human Model for Safety (THUMS) AM50 v6.1 and the Global Human Body Model Consortium (GHBMC) M50-O v6.0 in moderate-speed rear impact (ΔV of 24 km/h) and compares model head, cervical spine, and T1 kinematics to previously published PMHS data. An open-source finite element (FE) seat model was extracted from the 2012 Toyota Camry FE model developed by George Mason University. Sled acceleration data obtained during testing were used to drive simulated sled motion, and occupant kinematics were recorded. Normalised Root Mean Square Deviation (NRMSD) and cross-correlation methods outlined in ISO18571 were used to quantify differences in time-history data between PMHS and HBMs. The desired 10% threshold for average NRMSD was not met by either HBM for any of the response data evaluated. Average ISO rating showed fair biofidelity (THUMS = 0.62, GHBMC = 0.62) for both model response data compared to the two PMHS data sets available. Peak intervertebral rotations in the cervical spine trended similarly in both HBMs, with the best agreement in the upper levels. Study outcomes contribute to the understanding of the biofidelity of the head-neck responses of the HBMs seated on a production seat and subjected to moderate-speed rear impact.

***Keywords*** Cervical spine response, crashworthiness, Global Human Body Model Consortium, moderate-speed rear impact, Total Human Model for Safety.

## I. INTRODUCTION

Automotive rear impact resulting in whiplash has resulted in an enormous societal burden, costing an estimated $2.7 billion per year while affecting nearly 275,000 people annually in the USA alone [1]. Estimates across Europe place these numbers even higher, at an estimated €5–€10 billion per year [2]. With a switch to autonomous vehicles, non-standard seating configurations are likely to occur in future vehicles. One configuration currently under consideration by researchers places front-seat occupants in a rear-facing condition [3], which has the potential to expose the occupants to higher relative rear-impact conditions in the event of a forward collision. Many past whiplash research efforts have focused on low-speed (ΔV<20 km/h) impact conditions [4], but data are available to support the conclusion that there is also a risk for cervical spine injuries in moderate-speed rear impacts (ΔV=24 km/h). Previous research has shown a potential risk for flexion-related cervical spine injury in moderate-speed rear impact [5], differing from the typical hyperextension-related injuries expected. Therefore, it is important to develop adequate tools that can supplement PMHS research to determine injury risk in these specific environments that are capable of accurately capturing this experimentally observed injury mechanism.

Anthropomorphic Test Devices (ATDs), such as the BioRID II, have been specially designed for the evaluation of occupant kinematics in a rear impact. However, previous research suggests that there are still potential improvements that could be made to more accurately capture cervical spine kinematics observed in post-mortem human subjects (PMHS) during moderate-speed rear impacts [6], leaving a gap in capability if these data are required. Advanced development efforts of finite element (FE) Human Body Models (HBMs) by organizations such as Toyota Motor Corporation and the Global Human Body Models Consortium (GHBMC) have produced models such as the Total Human Model for Safety (THUMS) AM50 v6.1 and the GHBMC M50-O v6.0, respectively. Both models provide a detailed representation of a 50$^{th}$ percentile male occupant, including hard tissue and musculature attachments in the spine. These detailed models are now capable of providing data to supplement traditional experimentation using ATDs and PMHS, including gross body segment and detailed cervical spine kinematics. Initial model validation included head kinematics in low-speed rear impacts for THUMS [7] and cervical spine kinematics for GHBMC [8].

T. DeWitt (e-mail: dewitt.167@buckeyemail.osu.edu; tel: +19376721079) and V. Pradhan are PhD students and Y-S. Kang is an Associate Professor in The Ohio State University, Columbus, OH.

Subsequent research has been performed to evaluate cervical spine response in the THUMS model in a production seat, but again in low-speed rear-impact conditions [9]. Moderate-speed rear impact simulations have been performed with the GHBMC model to evaluate head and T1 kinematics, but these simulations were performed only with an experimental seat [10]. The purpose of the current study leverages the experimental work previously performed by Kang *et al*. [5-6] to evaluate both the GHBMC and the THUMS head and cervical spine kinematics in a moderate-speed (ΔV of 24 km/h) rear-impact scenario with a production seat, to determine model accuracy and to assess differences in model performance.

## II. METHODS

### *FE Sled Fixture*

An open-source 2012 Toyota Camry FE seat model created by the Center for Collision Safety Analysis at George Mason University [11] was used for all simulations. The seat model head restraint and seat-back stiffness were modified to better represent the 2011 Camry seat used in the PMHS study. Details on the seat modifications can be found in the Appendix. The seat model was constrained to a rigid sled floor using constrained extra nodes set at the seat anchor points. An acceleration was then applied using boundary-prescribed motion in the positive X-direction (10 g peak, ΔV of 24 km/h). The final seat model and sled pulse can be seen in Fig. 1.

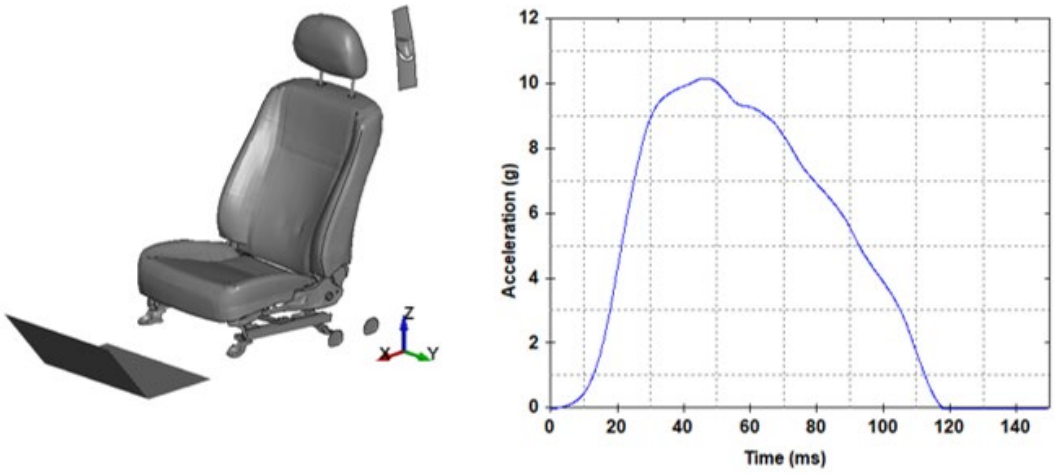


Fig. 1. (a) FE seat model and (b) assigned sled acceleration.

### *Positioning and Anthropometry*

Anthropometric measures were obtained during testing for each PMHS and critical values relating to head and neck response were identified and LS-Prepost was used to obtain equivalent measurements for each of the human body models. Anthropometric measurements for both HBMs and PMHS are also shown in Table I for comparison.

TABLE I
ANTHROPOMETRIC MEASUREMENTS

| Parameter | THUMS | GHBMC | PMHS1 | PMHS2 |
|---|---|---|---|---|
| Stature (cm) | 178.6 | 174.9 | 184 | 178 |
| Weight (kg) | 78.5 | 78.6 | 75.3 | 71.2 |
| Seated height (cm) | 89.6 | 92.1 | 83.0 | 80.0 |
| Sternum-Tragus length (cm) | 19.2 | 22.1 | 20.5 | 19.5 |
| Neck breadth (cm) | 11.9 | 12.1 | 9.2 | 11.3 |
| Neck depth (cm) | 11.9 | 13.9 | 13.0 | 10.7 |
| Neck circumference (cm) | 37.9 | 36.2 | 35.0 | 36.9 |

Positioning information for both HBMs was derived from FARO points taken during PMHS testing [5-6]. Anatomical landmarks were used to determine the subject head, neck, torso, pelvis, and lower extremity angles. These data were then used to guide the initial orientation of the models using Oasys Primer 18.1. All positioning targets can be found in Table II. The visual reference to all visible structures in the model is outlined in Fig. 2.

TABLE II
HBM POSITIONING TARGETS

| Body region | Target |
|---|---|
| Head ($\theta_1$) | 0.0° |
| Neck ($\theta_2$) | 13.5° |
| Torso ($\theta_3$) | 20.0° |
| Femur ($\theta_4$) | 15.0° |
| Tibia ($\theta_5$) | 45.0° |
| Pelvis (not shown above) | 32.0° |
| Backset | 50 mm |
| Topset | 80 mm |
| GT with respect to seat pivot z-position | 80 mm |

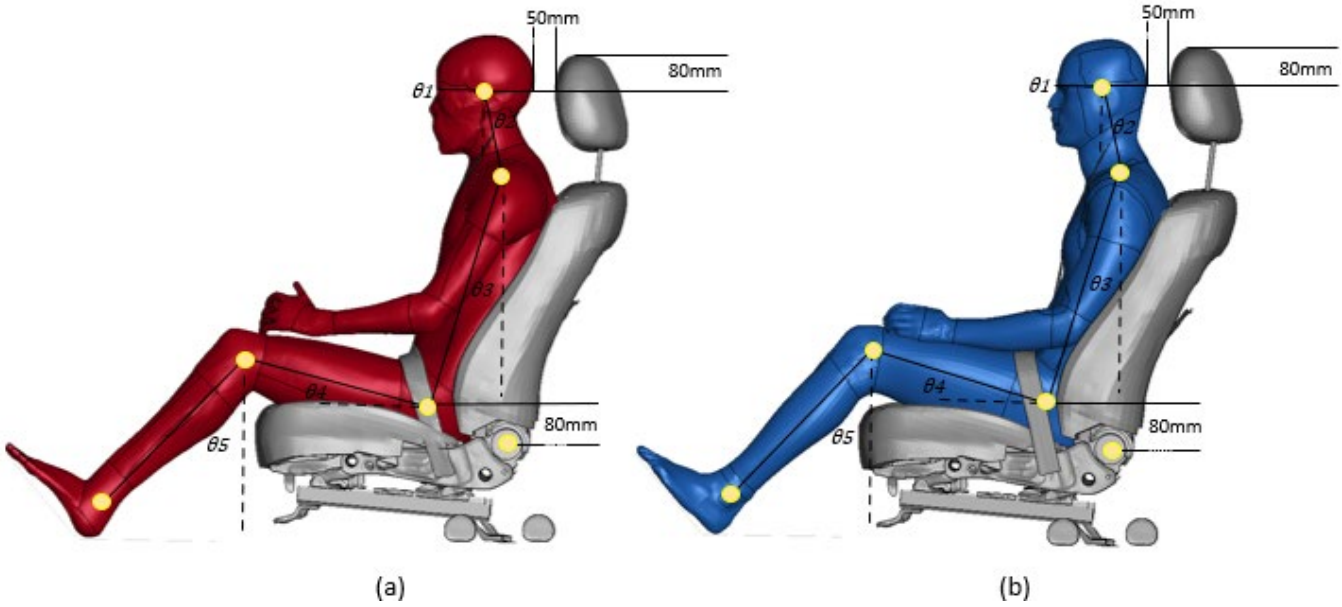


Fig. 2. HBM initial position for (a) THUMS and (b) GHBMC.

***HBM-Sled Integration***

After completion of the HBM segment orientation, LS-PrePost v4.7.17 was used to integrate the seat FE model with the HBMs. The load body keyword was used to settle the HBM into the final position within the seat in the X and Z direction. Head X-position with respect to the seat head restraint was used to determine the whole HBM final X-position in the seat. FARO data obtained during testing relating the seat pivot point to the subject's greater trochanter (GT) location were used to guide the final settled Z-position in the seat (target GT z-position = 80 mm). To limit body segment movement during settling simulations, single point constraints were created for the skeletal structure. For X settling simulations, constraints were set in Y, Z, RX, RY and RZ. For Z settling simulations, constraints were set in X, Y, RX, RY and RZ. The final head position with respect to head restraint was accomplished by adjusting head restraint height (target topset = 80 mm) and by moving the head using boundary-prescribed final geometry (target backset = 50 mm). Shoulder and lap belts were routed and anchored at the points highlighted in Fig. 3. To mimic the experimental static tension setup, element seat-belt retractors were added to the anchor points to allow for pre-tensioning of the belt before pulse initiation. Pretension values were set to 26.7 N and 17.8 N for the shoulder belt and lap belt, respectively. A 50 ms delay was added to the pulse initiation to allow time for belt tension to reach the initial set value.

Fig. 3. HBM position in seat and belt retractor locations.

A comparison of the final position for each HBM to PMHS seated position is shown in Fig. 4. All target angles were achieved within ± 2°. All desired distance references were achieved within ± 5 mm.

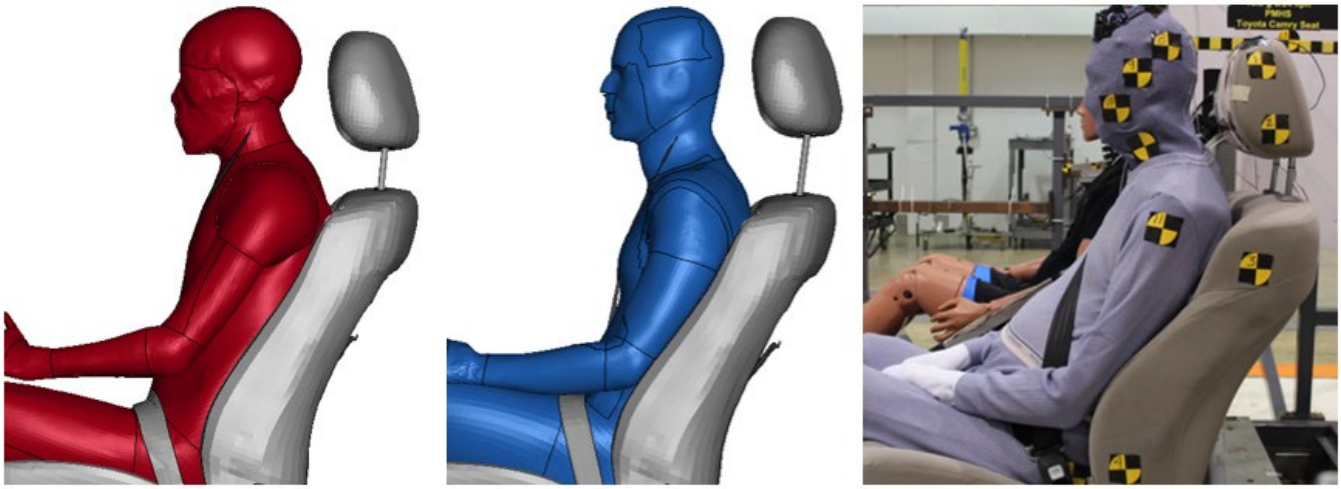

(a) (b) (c)

Fig. 4. Final seated position for (a) THUMS, (b) GHBMC and (c) PMHS.

***Data Analysis***

Occupant kinematics were evaluated for a duration of 180 ms after pulse initiation. An evaluation was based on accelerations at the head centre of gravity (CG) and T1 vertebral body, recorded in the same body-fixed coordinate system as PMHS. Peak intervertebral rotations about the y-axis of the cervical spine were also compared to experimental data in addition to rotation time histories of the head and T1. To quantify differences in time-history data, normalised root mean squared deviation (NRMSD) values were calculated using Equation (1):

$$NRMSD = \frac{\sqrt{\left(\frac{1}{n}\right)\sum_{i=1}^{n}(y_{HBM} - y_{PMHS})2}}{ymax_{PMHS} - ymin_{PMHS}} \quad (1)$$

Where $y_{HBM}$ is the human body model response at i, $y_{PMHS}$ is the observed PMHS response at i, $ymax_{PMHS}$ is the maximum value of the observed PMHS time history response and $ymin_{PMHS}$ is the minimum value of the

observed PMHS time history response. NRMSD values were calculated for model response compared to each PMHS response separately and these NRMSD values averaged for the final reported value.

Time-history data were also analyzed for cross correlation ratings using methods outlined in ISO18571. This method takes into account ratings for signal phase, magnitude and slope. Additional evaluation criteria outlined in this standard include ratings for corridors. However, the limited number of experimental data sets available was not sufficient for corridor generation. Since the final ISO rating is calculated using weight factors and all four variable scores (corridor, phase, magnitude, and slope), the weight factor for corridor was set to 0.0, and weight factors for each of the other parameters were evenly distributed at 0.33. Scores were calculated for each PMHS dataset and averaged for the final reported value. All local coordinate systems were oriented according to SAE-J211. Head accelerations were filtered using CFC1000 filter and all cervical spine and thoracic spine data were filtered using CFC180 filter.

## III. RESULTS

Gross kinematic response between both HBMs and PMHS trended similarly, with slight variations in event timing. As the pulse initiated, both HBMs moved slightly up the seat back until caught by the lap belt. The seat back was also pushed into a rearward rotation before ultimately springing the occupant forward. Initial head contact was made between the head of both HBMs approximately 80 ms after pulse initiation, compared to 66 ms for PMHS. Maximum excursion occurred 10 ms apart for the THUMS (120 ms) and GHBMC (130 ms), which were both slightly later than PMHS (105 ms). Head release of both PMHS from the head restraint occurred at ~185 ms, however GHBMC and THUMS head release from the head restraint occurred slightly sooner, at 165 and 170 ms, respectively.

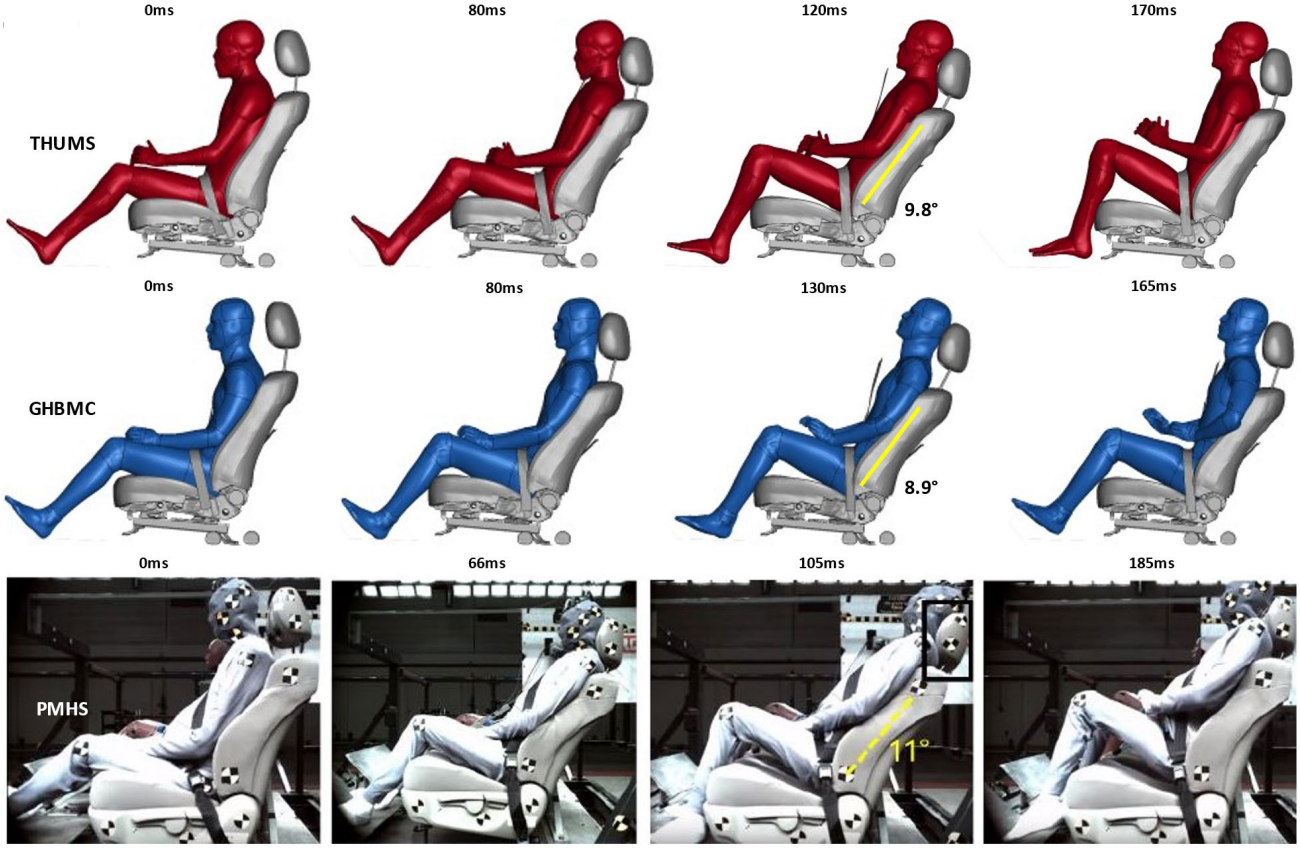


Fig. 5. Summary of key events, from left to right: initial position, initial head contact, maximum head excursion, head release from the head restraint.

Qualitative comparison of kinematics showed good agreement between both HBMs and PMHS for lower extremity, head and neck response. The upper extremity response of THUMS trended similarly to the PMHS, initially contacting the seatback and rebounding forward. GHBMC however, showed slipping of the humerus past the edge of the seatback. This could be due to slight differences in geometry in this region or slight differences in positioning relative to the edge of the seatback.

Linear accelerations in the x- and z-axis from the GHBMC and THUMS models were compared to two PMHS. Peak x-axis accelerations at the head were within the experimental PMHS range (16.1–17.7 g) for both models, however T1 peak x-accelerations were consistently low compared to PMHS (18.0–18.1 g) (Fig. 6).

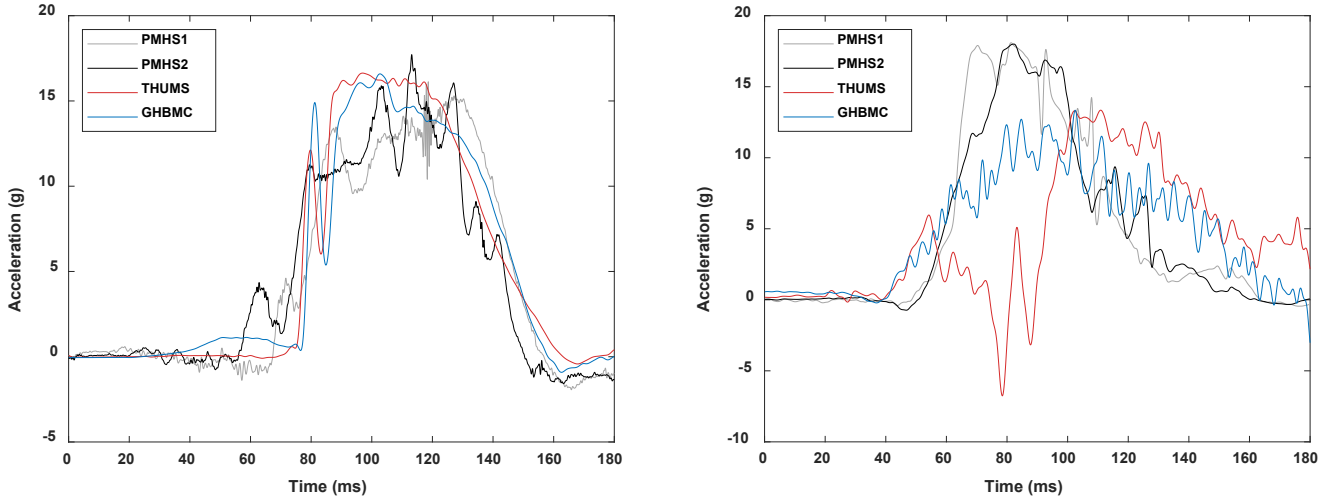


(a) (b)

Fig. 6. x-acceleration time-history for (a) head and (b) T1. Plot includes both THUMS and GHBMC HBMs as well as two PMHS data sets.

Head linear z-accelerations trended similarly in both THUMS and GHBMC at initial pulse onset, which was similar to PMHS1 data in negative peak acceleration magnitude (-6.2 g). Peak accelerations for the head were both slightly underpredicted compared to testing (11.4–16.2 g). Likewise, both HBMs trended similarly with respect to T1 z-acceleration up to approximately 80 ms after pulse initiation. After the 80 ms point, both pulses seemed to differ from experimental data with respect to pulse shape (Fig. 7), although the peak acceleration for the THUMS model was within the experimental range (5.9–10.8 g).

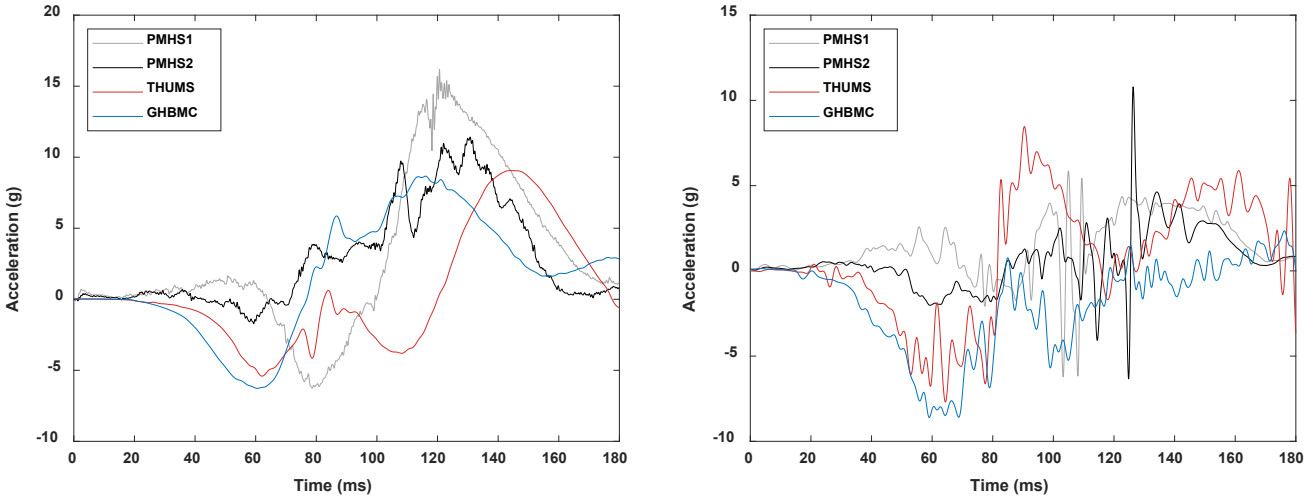


(a) (b)

Fig. 7. z-acceleration time-history for (a) head and (b) T1.

All recorded Y-rotations trended similarly between HBM and PMHS data. Peak head Y-rotation for both FE models fell within the experimentally determined range (26.2° to 57.4°) as did the negative peak head relative to T1 rotation (-20.2° to -30.8°). The model response seemed consistent with the PMHS response in that the main rotation for the head and T1 were rearward rotations. Both models tended to underpredict T1 rotation compared to PMHS (39.8° to 41.7°). The time histories of these kinematics are shown in Fig. 8.

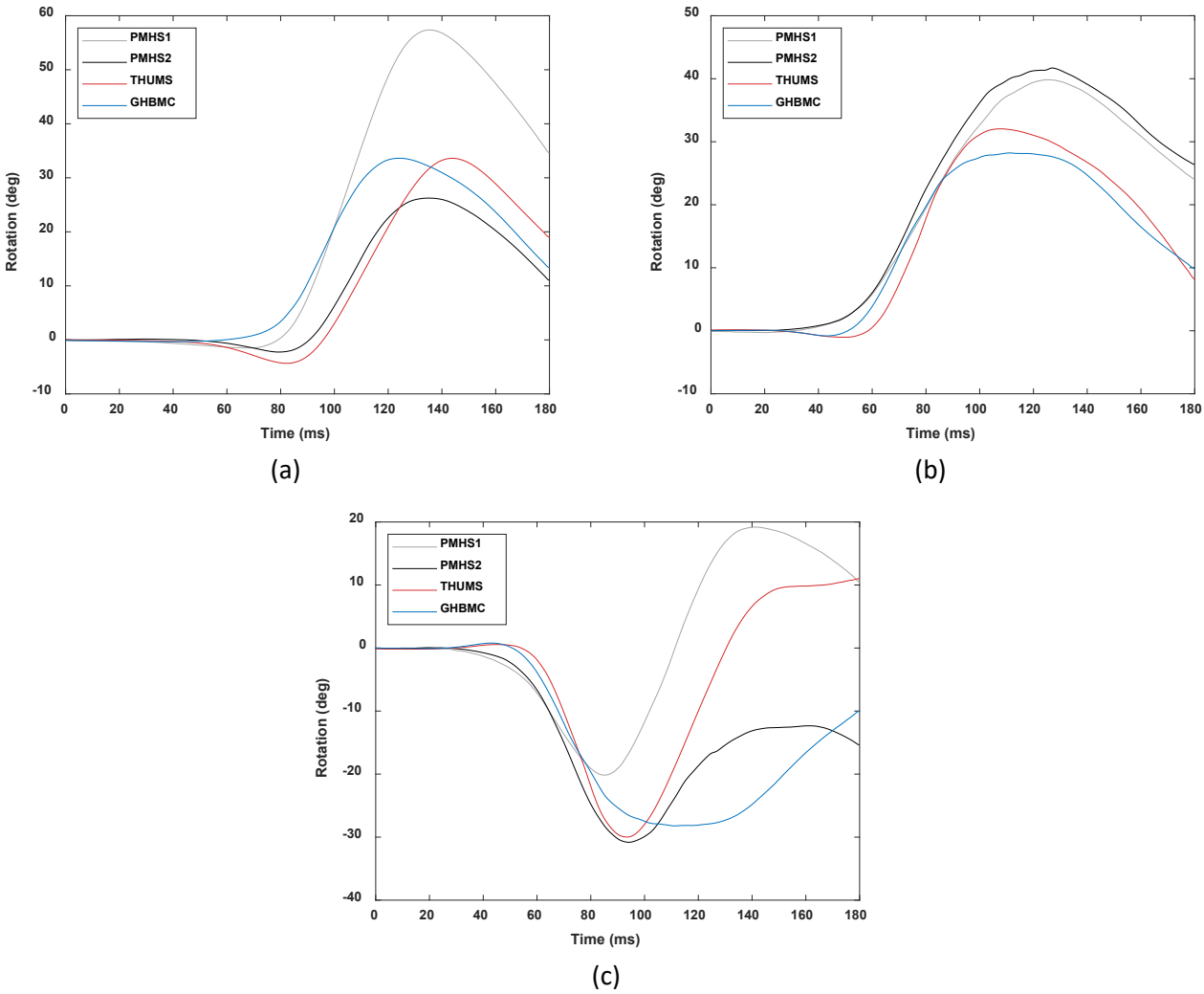


Fig. 8. (a) Head Y-rotation, (b) T1 Y-rotation, and (c) head relative to T1 Y-rotation.

To better quantify differences between the PMHS response and individual HBM response, NRMSD values and ISO scores were calculated for all metrics previously discussed and averaged for two PMHS tests. Peak responses, average NRMSDs, and ISO ratings are summarised in Table III.

TABLE III
SUMMARY OF AVERAGE NRMSD VALUES (%) ,ISO RATINGS AND PEAK RESPONSE DATA

| | Peak response | | | Average NRMSD (%) | | Average ISO Rating | |
|---|---|---|---|---|---|---|---|
| | THUMS | GHBMC | PMHS range | THUMS | GHBMC | THUMS | GHBMC |
| Head X-acceleration | 16.6 g | 16.6 g | 16.1–17.7 g | 12.6 | 11.9 | 0.73 | 0.69 |
| Head Z-acceleration | 9.1 g | 8.7 g | 11.4–16.2 g | 30.6 | 20.7 | 0.61 | 0.59 |
| T1 X-acceleration | 13.4 g | 13.3 g | 18.0–18.1 g | 39.6 | 18.8 | 0.44 | 0.52 |
| T1 Z-acceleration | 8.5 g | 2.35 g | 5.9–10.8 g | 24.1 | 30.0 | 0.35 | 0.40 |
| Head Y-rotation | 33.6° | 33.6° | 26.2° to 57.4° | 20.8 | 23.5 | 0.75 | 0.75 |
| T1 Y-rotation | 32.1° | 28.2° | 39.8° to 41.7° | 19.3 | 22.2 | 0.81 | 0.78 |
| Head relative to T1 Y-rotation | -30.0° | -28.2° | -20.2° to -30.8° | 32.1 | 38.8 | 0.63 | 0.64 |

Tables showing the individually calculated ISO ratings for each PMHS and individual ratings for phase, magnitude, and slope can be found in the Appendix.

Peak intervertebral rotations at C2C3, C4C5, C5C6, C6C7 and C7T1 were also determined to quantify cervical spine kinematics. The intervertebral motion was measured using locally defined coordinate systems created on the vertebral bodies. In general, cervical spine extension was overpredicted by both HBMs when compared to the experimental data and tended to underpredict flexion at the lower (C4-T1) vertebral levels. These results are summarised in Fig. 9. Positive values indicate relative rearward rotation at the indicated level, and negative values indicate forward rotation.

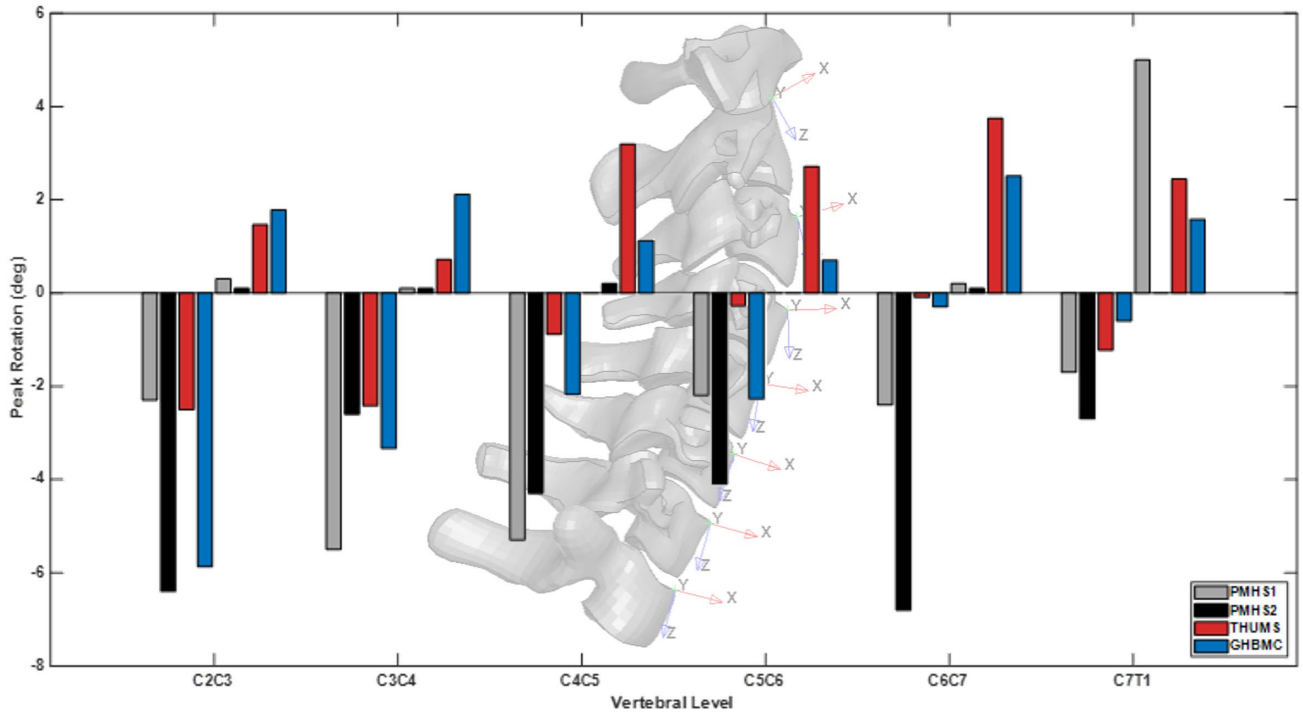


Fig. 9. Peak intervertebral rotations about y for C2C3, C4C5, C5C6, C6C7 and C7T1.

## IV. DISCUSSION

Anthropometric measurements between both HBMs and PMHS varied slightly; however, they were within a reasonable range for measurements expected to contribute to the model response. Both HBMs estimated seated height was slightly higher than PMHS (80cm – 83cm). No direct measurement of neck length was taken, but a comparison can be made using the recorded Sternum-Tragus length, in which both models were within ~10% of the average for the PMHS. Neck circumference measurements were also reasonably close, with each model being within ~7% of the average for the PMHS. Total weights of both HBMs were higher than each of the PMHS but was again within ~7% of the average PMHS weight.

Gross kinematics between HBMs and PMHS trended similarly, with slight variations in event timing. Initial head contact between HBMs was consistent at 80 ms but was slightly later than the 60-70 ms seen in PMHS testing. This could indicate a slightly stiffer response of the HBM neck compared to the PMHS. Peak head accelerations at the time of initial head contact were also inconsistent between simulation results and PMHS data. Simulation results suggest 3-4 times the acceleration level experienced during the experimental study. This could likely indicate a need for improved foam material model in the head restraint, which was not considered as part of this study. GHBMC had the lowest seat-back rotation, which could explain the earliest head release from the head restraint observed between HBMs and PMHS. All maximum seat-back rotations were within a reasonable range, with PMHS = 11°, THUMS = 9.8° and GHBMC = 8.9°.

NRMSDs comparing HBM response to PMHS response showed closer agreement with the GHBMC model for head acceleration (x and z), T1 x-acceleration, and head Y-rotation. THUMS response had a better agreement for both head Y-rotation, head relative to T1 Y-rotation and T1 z-acceleration compared to GHBMC. However, all of the NRMSDs for both models were above the desired 10% threshold. Average cross correlation ratings for GHBMC showed fair biofidelity for all time-history response data other than T1 z-acceleration. For THUMS, the T1 Y-rotation received a good biofidelity rating, while Head Y-rotation, Head-to-T1 Y-rotation, Head x and z-

acceleration received fair scores and T1 x and z-acceleration showed poor biofidelity.

The resultant acceleration of T1 was also investigated to determine if local coordinate axis orientation could be a potential reason for discrepancies in accelerations. However, peak values were still consistently underpredicted by both HBMs, suggesting other potential influences as the root cause.

The initial position of the T1 vertebral bodies for THUMS and GHBMC were measured in relation to a node horizontal to the posterior-most point on the spinous process to the head restraint post in X to determine any variation in an initial position not accounted for by neck angle, torso angle, and head backset. It was found that the T1 vertebral body for GHBMC was ~10 mm closer to the seat structure than THUMS, which may explain the more consistent onset in acceleration observed in the GHBMC acceleration data. It may also be important to consider differences in foam material properties between the production seat and the FE model, as the current seat model response has not been extensively validated in this scenario and would likely influence T1 acceleration given the potential for interaction.

Head and T1 kinematics were evaluated previously in moderate-speed rear impact in an experimental seat by Katagiri *et al*. [10], in which similar observations were made on the underprediction of T1 accelerations and Y-rotation. Biofidelity Ranking System (BRS) scores showed better agreement between PMHS and GHBMC for T1 data than head data in this study. Utilizing average NRMSD, this was true for the rotation data, but not acceleration data, in the experimental setup we explored, in which head x had the lowest NRMSD of any channel. Interestingly, these low NRMSD values did not correspond to the highest ISO rating, which was found for T1 rotation in both HBMs. Looking further into this it was found that the calculated slope rating for head x acceleration was low for each model, reducing the overall cross-correlation rating.

To determine a potential cause for differences in head rotation comparison was made between PMHS mass properties collected during testing and approximate values extracted from the HBMs. The PMHS reference values were given with respect to the head anatomical coordinate system developed using the tragion, and infraorbital notch locations. Because the HBMs do not have representation for the tragions and the centre of these points (left and right) becomes the origin for the local coordinate system, an approximation was made, and a reference node was used on the superior portion of the condylar process of the mandible. Weight estimations for the head were established using the mass trimming tool within LS-PrePost and by selecting only parts superior to the C2 vertebral body. Any parts that extended below this region, such as the neck flesh and muscle, were excluded entirely. PMHS recorded range for head mass was 3.75–4.00 kg. Both HBMs' head masses were over these values, falling in at 4.10 kg (GHBMC) and 5.48 kg (THUMS). CGx data fell reasonably close for both models compared to PMHS, however GHBMC CGz was approximately 10 mm higher in z compared to the highest CGz recorded for PMHS. Differences in these mass properties may have contributed to the differences in kinematics observed in both the head and subsequent neck response. A summary of these data and mass moment of inertia data is shown in Table IV.

TABLE IV
SUMMARY OF PMHS AND HBM HEAD MASS PROPERTIES

| | PMHS1 | PMHS2 | THUMS | GHBMC |
|---|---|---|---|---|
| Head Mass (kg) | 3.75 | 4.00 | 5.48 | 4.10 |
| Ixx $(kg * mm^2)$ | 18673.7 | 13033.9 | 23953.5 | 17078.8 |
| Iyy $(kg * mm^2)$ | 17591.8 | 19020.4 | 30261.1 | 20633.9 |
| Izz $(kg * mm^2)$ | 12428.9 | 17864.3 | 23619.9 | 15345.7 |
| CGx (mm) | 9 | 2.9 | 7.36 | 0.37 |
| CGz (mm) | -21.9 | -24.5 | -20.7 | -34.8 |

Intervertebral rotations showed close agreement in C2C3 and C3C4 flexion but varied greatly in most other cases. Individual trends in flexion vs. extension between levels were also incorrectly predicted in some cases, such as that seen at C6C7, again indicating a potential area for improvement in both FE models. Differences in material properties controlling joint stiffnesses within the model may be a good point for further investigation. It may also be important to consider detailed vertebral body orientations as initial boundary conditions. Variations in cervical spine curvature and overall cervical spine length were noted between GHBMC and THUMS and are Illustrated in Fig. 10. HBM total cervical spine length was estimated by summing individual vertebral body height

measurements made on the anterior face of the bodies from C1 – C7. No information was available for positioning of the individual vertebral bodies in the cervical spine and was therefore determined through the positioning of the head and torso. Given that in-position X-ray images were not taken, data for PMHS was not available for comparison, but it's reasonable to assume variation would also exist both in size and initial orientation both between subjects and HBMs. Variation in individual vertebral body shape and initial orientation could contribute to peak measured flexion/extension values if structures, such as the spinous processes and facet joints, were to interact with an adjacent."

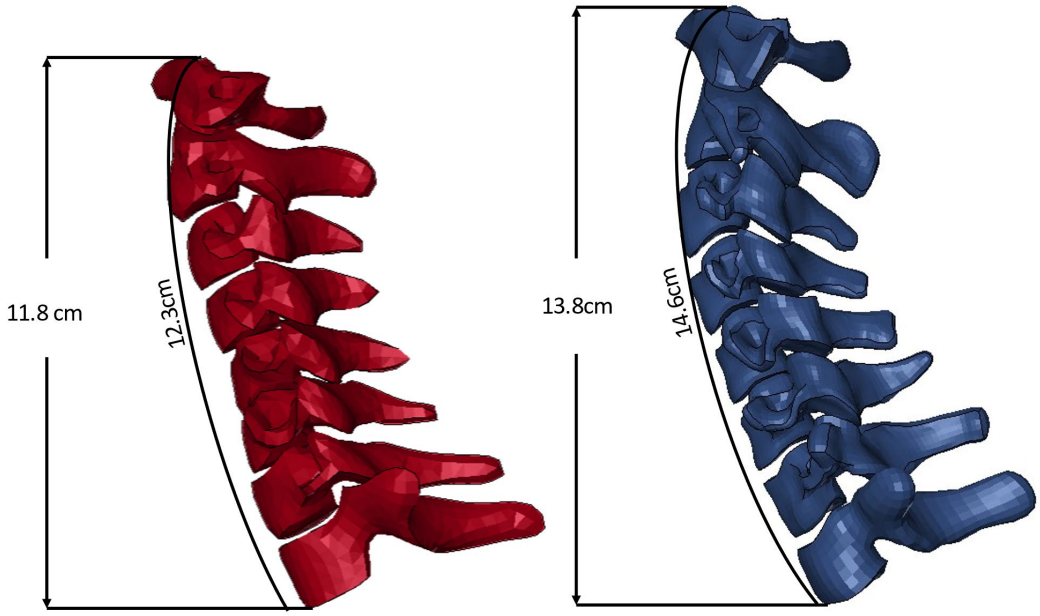


Fig. 10: Comparison of THUMS and GHBMC cervical spine

Noticeable differences in model skull geometry between HBMs and PMHS, specifically in the posterior region, may have also affected the model responses given that the main responses were from the head-to-head restraint interaction. The THUMS model has a very pronounced curvature in the posterior crown of the skull that could have a significant effect on how it interacts with the head restraint and influence intervertebral body kinematics. These differences are highlighted in Fig. 11 between the two human body models and in Fig. 12 in the appendix for the PMHS.

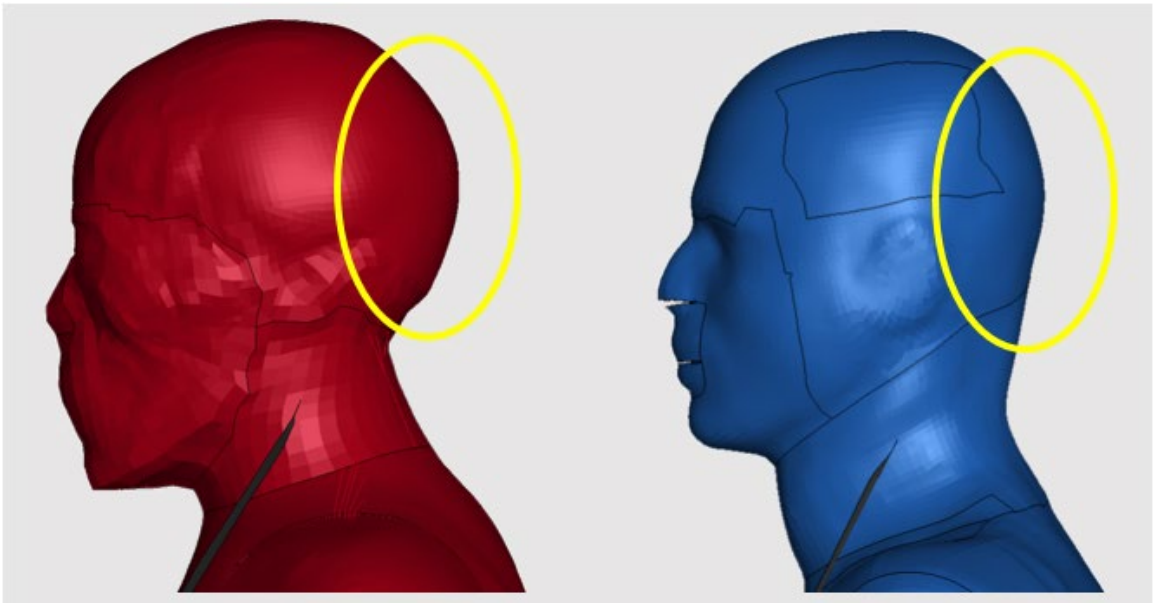

**Fig. 11. Differences in skull geometry between THUMS and GHBMC.**

***Limitations***

It should be noted that variations in PMHS response were also observed in both intervertebral rotation data and measured acceleration data, which could have added to the calculated error in the HBM response. Additional PMHS response data for comparison would strengthen these results given the current data set consisted of only two PMHS. This study should therefore be used only as an initial look into this use case for these HBMs and used to guide further model evaluation when additional experimental data is available. Future experimental work related to this should attempt to accurately document initial cervical spine orientation, as this may be important when evaluating intervertebral body kinematics. Initial cervical spine vertebral body orientation information was not captured in the study used for this analysis, so only gross segment positioning data were used to guide HBM setup. Future modeling work may include sensitivity analysis to determine these effects, although this variation would likely also be present in experimental subject data as well. Corridors for spinal curvature from experimental studies would also be useful in ensuring the accuracy of the model setup.

"It should also be noted that initial simulations to settle the HBMs into the seat were performed to allow for initial contact and accurate occupant positioning based on data recorded during experiments. Nodal coordinates after each positioning and settling simulation for the HBMs were updated however, any developed stress/strain within the elements were not carried over between simulations. An additional study to determine what effect, if any, these initial stresses from HBM settling have on the subsequent model response should be performed as future work before consideration to model changes and model validation."

The FE seat model used in this study has also not been fully validated for use in these types of experiment. Initial validation was performed to validate seat-back rotation using a Hybrid III ATD (see Appendix B), as this was believed to be a key contributor to occupant response that could be evaluated with existing data. ATD testing was chosen to minimize the variability seen in PMHS thorax, head, and neck mass and experimental response. Seat back structure stiffness was tuned to match the experimental seat back rotation data available and this optimized model was used in the simulations discussed here. ATD response data was not used for comparison however, which should be the focus of future seat response validation efforts. Parameters influencing overall structural response, such as seat deformation, foam compression and occupant-to-seat friction, have the potential to greatly influence occupant kinematics and may explain some of the discrepancies in peak acceleration and acceleration onset seen during this study. Additional work to validate the seat response and ATD response and/or material testing to ensure appropriate foam model response would ensure accurate boundary conditions for comparison to PMHS testing and should be the focus of future work before consideration for HBM model response optimization.

## V. CONCLUSIONS

This study aimed to evaluate the head and cervical spine kinematics of both the GHBMC M50-O v6.0 and the THUMS AM50 v6.1 in a moderate-speed rear impact. Calculated average NRMSD values were found to exceed 25% in head x-, T1 x- and z-accelerations, Head Y-rotation, and head relative to the T1 Y-rotation for the THUMS model and in T1 z-acceleration and head relative to the T1 Y-rotation for GHBMC. GHBMC showed slightly better agreement to experimental data than THUMS in most cases evaluated, but neither model was able to fall within the desired 10% NRMSD threshold for any parameter measured nor did they accurately predict cervical vertebral kinematics at all levels. Alternative comparison performed using methods outlined in ISO18571 resulted in an average overall score of fair biofidelity for both human body models when compared to the existing PMHS data. The current study is limited in that only two subject data sets were available for comparison to the model outcomes, and therefore corridor development for PMHS response was not possible. Notable variability between the existing PMHS data suggests that additional PMHS data for this condition is required to better quantify subject variability and to develop appropriate response corridors. The results from this study demonstrated significant differences in model responses compared to the existing data. However, definitive conclusions on HBM fidelity could not be drawn until additional PMHS data is available to accurately quantify variation in experimental response. The outcomes of this study will contribute to a better understanding of the biofidelity of the head-neck responses of both the THUMS and GHBMC models seated on a production seat and subject to a moderate-speed rear impact.

## VI. ACKNOWLEDGMENTS

We would like to thank all of the faculty, staff and students of the Injury Biomechanics Research Center for their support with this and future work.

## VII. REFERENCES

[1] "National Highway Traffic Safety Administration, 49 CFR Part 571 and 585" (2007) Internet: https://www.govinfo.gov/content/pkg/FR-2007-05-04/pdf/07-2011.pdf, May 2007 [Accessed February 2023].

[2] EEVC (2007) Dummy Requirements and Injury Criteria for a Low-speed Rear Impact Whiplash Dummy, Working group 12 report, 2007.

[3] Jorlov, S., Bohman, K., Larsson, A. (2017) Seating Positions and Activities in Highly Automated Cars, A Qualitative Study of Future Automated Driving Scenarios. *Proceedings of the IRCOBI Conference*, 2017, Antwerp, Belgium.

[4] Svensson, M., Bermond, F. *et al*. (2002) EEVC European Enhanced Vehicle-safety Committee Ad-Hoc Group on Whiplash Injuries and EEVC WG12 Advanced Anthropometric Adult Crash Dummies, 2002.

[5] Kang, Y. S., Moorehouse, K., Icke, K., Herriott, R., Bolte, J. (2014) Head and Cervical Spine Response of Post Mortem Human Subjects in Moderate Speed Rear Impacts. *Proceedings of the IRCOBI Conference,* 2014, Berlin, Germany.

[6] Kang, Y. S., Moorehouse, K., Icke, K., Herriott, R., Bolte, J. (2015) Rear Impact Head and Cervical Spine Kinematics of BioRID II and PMHS in Production Seats. *Proceedings of the IRCOBI Conference,* 2015, Lyon, France.

[7] Toyota Motor Corporation (2021) Documentation, Total Human Model for Safety, AM50 Occupant Model Version 6.1.

[8] Elemance LLC (2021) Global Human Body Models Consortium User Manual: M50 Detailed Occupant Version 6.0 for LS-DYNA®.

[9] Kitagawa, Y., Yamada, K., Motojima, H., Yasuki, T. (2015) Consideration on Gender Difference of Whiplash Associated Disorder in Low Speed Rear Impact. *Proceedings of the IRCOBI Conference,* 2015, Lyon, France.

[10] Katagiri, M., Zhao, J., Lee, S., Moorhouse, K., Kang, Y.S. (2019) Biofidelity Evaluation of GHBMC Male Occupant Models in Rear Impacts. *Proceedings of the IRCOBI Conference*, 2019, Florence, Italy.

[11] George Mason University (2016) Tech Summary: Development and Validation of a Finite Element Model for the 2012 Toyota Camry Passenger Sedan. Internet:[ https://www.ccsa.gmu.edu/models/2012-toyota-camry/], May 2016 [Accessed March 2023].

## VII APPENDIX A

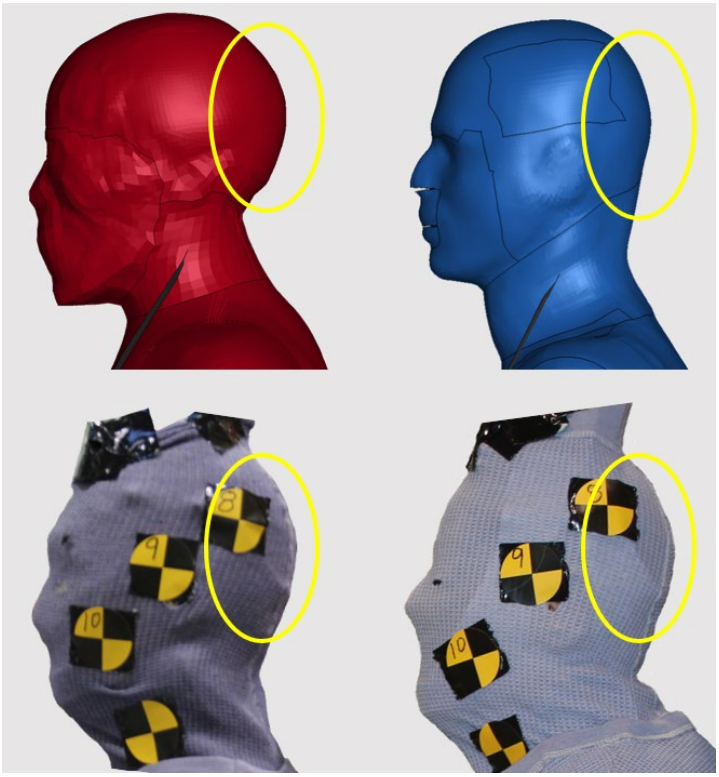

Fig. A1: Comparison of THUMS, GHBMC and PMHS skull geometries

TABLE AI
CALCULATED ISO RATINGS FOR GHBMC TO PMHS1

| Kinematic | Phase Rating (Ep) | Magnitude Rating (Em) | Slope Rating (Es) | Cross-Correlation Rating (R) |
|---|---|---|---|---|
| Head Y-Rotation | 0.98 | 0.29 | 0.79 | 0.68 |
| T1 Y-Rotation | 0.99 | 0.57 | 0.84 | 0.79 |
| Head-to-T1 Y-Rotation | 0.94 | 0.00 | 0.50 | 0.48 |
| Head x-Acceleration | 1.00 | 0.83 | 0.30 | 0.70 |
| T1 x-Acceleration | 1.00 | 0.55 | 0.00 | 0.51 |
| Head z-Acceleration | 1.00 | 0.58 | 0.34 | 0.63 |
| T1 z-Acceleration | 1.00 | 0.00 | 0.19 | 0.39 |

TABLE AII
CALCULATED ISO RATINGS FOR GHBMC TO PMHS2

| Kinematic | Phase Rating (Ep) | Magnitude Rating (Em) | Slope Rating (Es) | Cross-Correlation Rating (R) |
|---|---|---|---|---|
| Head Y-Rotation | 0.98 | 0.62 | 0.88 | 0.82 |
| T1 Y-Rotation | 0.99 | 0.46 | 0.85 | 0.76 |
| Head-to-T1 Y-Rotation | 0.96 | 0.95 | 0.54 | 0.81 |
| Head x-Acceleration | 1.00 | 0.82 | 0.24 | 0.68 |
| T1 x-Acceleration | 1.00 | 0.61 | 0.00 | 0.53 |
| Head z-Acceleration | 1.00 | 0.33 | 0.33 | 0.55 |
| T1 z-Acceleration | 1.00 | 0.00 | 0.24 | 0.41 |

TABLE AIII
AVERAGED CALCULATED ISO RATINGS FOR GHBMC TO PMHS1 AND PMHS2

| Kinematic | Phase Rating (Ep) | Magnitude Rating (Em) | Slope Rating (Es) | Cross-Correlation Rating (R) |
|---|---|---|---|---|
| Head Y-Rotation | 0.98 | 0.46 | 0.84 | 0.75 |
| T1 Y-Rotation | 0.99 | 0.52 | 0.85 | 0.78 |
| Head-to-T1 Y-Rotation | 0.95 | 0.48 | 0.52 | 0.64 |
| Head x-Acceleration | 1.00 | 0.83 | 0.27 | 0.69 |
| T1 x-Acceleration | 1.00 | 0.58 | 0.00 | 0.52 |
| Head z-Acceleration | 1.00 | 0.46 | 0.34 | 0.59 |
| T1 z-Acceleration | 1.00 | 0.00 | 0.22 | 0.40 |

TABLE AIV
CALCULATED ISO RATINGS FOR THUMS TO PMHS1

| Kinematic | Phase Rating (Ep) | Magnitude Rating (Em) | Slope Rating (Es) | Cross-Correlation Rating (R) |
|---|---|---|---|---|
| Head Y-Rotation | 0.98 | 0.28 | 0.83 | 0.69 |
| T1 Y-Rotation | 0.99 | 0.73 | 0.76 | 0.82 |
| Head-to-T1 Y-Rotation | 0.98 | 0.40 | 0.80 | 0.72 |
| Head x-Acceleration | 1.00 | 0.84 | 0.42 | 0.75 |
| T1 x-Acceleration | 0.99 | 0.29 | 0.10 | 0.46 |
| Head z-Acceleration | 1.00 | 0.57 | 0.33 | 0.63 |
| T1 z-Acceleration | 1.00 | 0.00 | 0.09 | 0.36 |

TABLE AV
CALCULATED ISO RATINGS FOR THUMS TO PMHS2

| Kinematic | Phase Rating (Ep) | Magnitude Rating (Em) | Slope Rating (Es) | Cross-Correlation Rating |
|---|---|---|---|---|
| Head Y-Rotation | 0.98 | 0.69 | 0.81 | 0.82 |
| T1 Y-Rotation | 0.99 | 0.63 | 0.79 | 0.80 |
| Head-to-T1 Y-Rotation | 0.99 | 0.00 | 0.65 | 0.54 |
| Head x-Acceleration | 1.00 | 0.79 | 0.39 | 0.72 |
| T1 x-Acceleration | 0.99 | 0.27 | 0.00 | 0.42 |
| Head z-Acceleration | 1.00 | 0.49 | 0.32 | 0.60 |
| T1 z-Acceleration | 1.00 | 0.00 | 0.01 | 0.33 |

TABLE AVI
AVERAGED CALCULATED ISO RATINGS FOR THUMS TO PMHS1 AND PMHS2

| Kinematic | Phase Rating (Ep) | Magnitude Rating (Em) | Slope Rating (Es) | Cross-Correlation Rating |
|---|---|---|---|---|
| Head Y-Rotation | 0.98 | 0.49 | 0.82 | 0.75 |
| T1 Y-Rotation | 0.99 | 0.68 | 0.78 | 0.81 |
| Head-to-T1 Y-Rotation | 0.99 | 0.20 | 0.73 | 0.63 |
| Head x-Acceleration | 1.00 | 0.82 | 0.41 | 0.73 |
| T1 x-Acceleration | 0.99 | 0.28 | 0.05 | 0.44 |
| Head z-Acceleration | 1.00 | 0.53 | 0.33 | 0.61 |
| T1 z-Acceleration | 1.00 | 0.00 | 0.05 | 0.35 |

## VIII. APPENDIX B

### A. *Matching the Head Restraint Geometry of the FE Seat to the Physical Seat*

The geometry of the head restraint of the production seat (2011 Toyota Camry) used in Kang's studies [5-6] (Fig. A1(a)) was different from the head restraint of the FE seat model used for this study. The head restraint of the seat model was therefore morphed into a 3D scan of the head restraint of the 2011 Toyota Camry seat to 15ptimizi discrepancy in boundary conditions between the experiments and simulations (Fig. A1(b)).

(a) (b)

Fig. B1. Matching the head restraint geometry of the FE seat to the physical seat: (a) 2011 Toyota Camry seat used in PMHS studies and (b) modification of the head restraint of the 2012 Toyota Camry FE model.

### B. *Optimising Seatback Rotation of the FE Seat*

The FE model of the seat has not been previously validated for rear impact. To build more confidence in response comparisons between the PMHS and the HBMs, it was necessary to perform a preliminary seat validation by 15ptimizing the seatback rotation, which is a crucial boundary condition for this study. FE models of Anthropomorphic Test Devices (ATDs) are frequently used for seat validation because of their geometrical similarity with their physical counterparts. In-house data were available from sled tests conducted at the Transportation Research Center Inc with the Hybrid-III ATD in the same loading condition as the PMHS. Simulations were run with LSTC Hybrid-III FE model seated on the FE seat model. An initial simulation with the Hybrid III FE model achieved a 9-degree higher seatback rotation compared to the experiments. The seatback frame in the FE model was subsequently modified by stiffening up the stress vs. strain curves used in the plastic material model (MAT24). The difference in seatback rotation between the modified FE seat model and the physical seat was 2 degrees, indicating improvement with respect to the initial simulation (Fig. A2). The modified FE seat was used for simulations with the THUMS and GHBMC models.

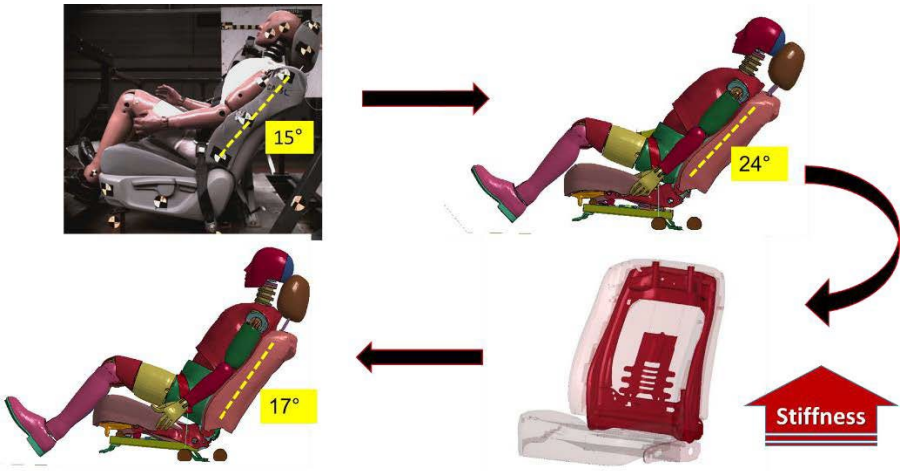


Fig. B2. Flow of events involved in 15optimizing seatback rotation of the FE seat using Hybrid III FE model.